

Rollins College

Rollins Scholarship Online

Student-Faculty Collaborative Research
Publications

Student-Faculty Collaborative Research

5-16-2023

The behavior of standing waves near the end of an open pipe with low mean flow

Thomas R. Moore

Makayle S. Kellison

Whitney Coyle

Follow this and additional works at: https://scholarship.rollins.edu/stud_fac

The behavior of standing waves near the end of an open pipe with low mean flow

Thomas R. Moore,^{a)} Makayle S. Kellison, and Whitney L. Coyle 

Department of Physics, Rollins College, Winter Park, Florida 32789, USA

tmoore@rollins.edu, mkellison@rollins.edu, wcoyle@rollins.edu

Abstract: The acoustic standing wave near the end of an open pipe is investigated using spectrally analyzed high-speed transmission electronic speckle pattern interferometry. It is shown that the standing wave extends beyond the open end of the pipe and the amplitude decays exponentially with distance from the end. Additionally, a pressure node is observed near the end of the pipe in a position that is not spatially periodic with the other nodes in the standing wave. A sinusoidal fit to the amplitude of the standing wave inside the pipe indicates that the end correction is well predicted by current theory. © 2023 Author(s). All article content, except where otherwise noted, is licensed under a Creative Commons Attribution (CC BY) license (<http://creativecommons.org/licenses/by/4.0/>).

[Editor: Charles C. Church]

<https://doi.org/10.1121/10.0019500>

Received: 29 March 2023 Accepted: 1 May 2023 Published Online: 16 May 2023

1. Introduction

The behavior of acoustic standing waves at the termination of an open pipe has been studied for centuries. Understanding the nature of these waves is important for many applications, and studies have been performed in contexts ranging from industrial applications to musical instruments.

In the simplest approximation, the open end of a pipe is considered to be the location of a node of an acoustic standing wave inside the pipe. It is well known, however, that the frequency of the standing wave inside the pipe indicates that the acoustic length of the pipe is greater than its physical length. This difference between the physical length and acoustic length is attributable to the nonzero acoustic impedance of the atmosphere outside the pipe. The reactive part of the atmospheric impedance induces a phase shift of the wave reflected from the end of the pipe, and this phase shift leads to an acoustic length that exceeds the physical length with a commensurately lower resonance frequency than is predicted by assuming that the final node occurs at the end of the pipe. This effect has led to the concept of the end correction, a length that is added to the physical length of the pipe to predict the correct resonance frequency of a standing wave inside the pipe.

The identification of the end correction dates back to at least 1877 when it was noted by Rayleigh.¹ All of the subsequent investigations of the effect appear to be experimental until 1948, when Levine and Schwinger proposed a theory that predicted the value of the end correction for a thin-walled pipe open to the atmosphere.² This theory predicted that the end correction for a long-wavelength low-frequency pipe resonance is $0.6133a$, where a is the pipe radius, which was in agreement with previously published experimental values. Further work in the second half of the 20th century and the early 21st century has led to a more complete understanding of the behavior of acoustic standing waves at the end of an open pipe, including accounting for different end conditions and the presence of flowing gas.^{3–6}

Here, we report experimental observations of the acoustic standing wave in an open pipe using a recently developed variation on transmission electronic speckle pattern interferometry (TESPI).⁷ This method produces images of standing waves inside a transparent pipe in the presence of flowing gas, enabling a close observation of the standing wave in a pipe initiated by oscillations from gas flowing over a sharp edge. Studying this type of oscillation in the presence of a flowing gas allows for observation of the acoustic standing wave inside of and beyond the end of the pipe. Using TESPI, we have observed the presence of the standing wave outside of the pipe as well as an internal acoustic node near the pipe end, which is not spatially periodic with respect to the other nodes in the standing wave.

2. Experimental procedure

To study the standing wave inside of a pipe with an open end, the fipple of an organ pipe was three-dimensionally (3D) printed with dimensions similar to those of an existing wooden organ pipe. The printed fipple was fit with a transparent square pipe having internal dimensions of 12.7 mm on each side. The length of the entire resonating cavity was

^{a)} Author to whom correspondence should be addressed.

approximately 36 cm, with a transparent region of approximately 25 cm. The imaging system is described in detail elsewhere,⁷ but it is useful to briefly outline the process to ensure that the data presented here are understandable.

The TESPI process depends on detecting a change in the optical path length of coherent light from a laser that propagates through the transparent pipe in a direction perpendicular to the flow. To enhance the optical effect, the flowing gas in the experiments described here was Freon R152a (1,1-difluoroethane) instead of air. The light propagating through the flow is then combined with coherent light from a reference beam that did not propagate through the flow. The speckle pattern produced by combining the two beams is captured by a high-speed digital camera with an acquisition rate of 9.9 kHz and fitted with a commercially available zoom lens. The images are then stored for later analysis.

The pressure variations created by the standing wave inside the pipe cause the gas to compress, creating a periodic spatial and temporal change in the optical path length of the light propagating through the pipe. The change in the optical path length is linearly proportional to the pressure of the gas, hence, the optical path length of the light changes with the oscillating pressure of the standing wave. A time-averaged image of the standing wave is obtained by filtering the images from the high-speed camera at the frequency of the acoustic standing wave. An image of the final 22.5 cm of the standing wave within the pipe oscillating in the eighth longitudinal mode is shown in Fig. 1(a). The image in Fig. 1(a) was produced by spectrally filtering 4096 images at the resonance frequency of 2.90 kHz.

The pixels in the image that are inside the pipe can be averaged in the direction perpendicular to the flow to produce a graph of the amplitude of the acoustic standing wave. This is displayed in Fig. 1(b) along with a fit to a sine function modified by a Gaussian envelope using a Levenberg-Marquart algorithm. The Gaussian envelope is necessary to account for the variation in the intensity of the laser beam. While there is significant noise in the measurement of the pressure amplitude, which is a by-product of the random nature of optical speckle, the fit results in an uncertainty in the wavelength of less than 1%. The distances on the horizontal axis in Fig. 1(b) are measured from the end of the pipe and, as expected, the fit indicates that the final node of the standing wave occurs outside the pipe. The distance from the end of the pipe to the position of the external node of the standing wave, as determined by the sinusoidal fit to the data, is $\Delta L = 0.66a \pm 0.04a$.

To investigate the behavior of the standing wave at the end of the pipe, the final 2 cm of the pipe were imaged. An image of the standing wave at the end of the pipe is shown in Fig. 2(a), where the extension of the standing wave beyond the end of the pipe is obvious. Surprisingly, there is also a node of the standing wave inside the pipe near the end. This can also be observed in Fig. 1(a), although it is less obvious. Averaging the pixel values inside the pipe in Fig. 2(a) results in the graph depicted in Fig. 2(b). The vertical line indicates the end of the pipe, which occurs after the internal node and before the end of the standing wave outside of the pipe. The curve in Fig. 2(b) is an exponential fit to the final 8 mm of the detectable standing wave.

3. Discussion

The functional fit shown in Fig. 1(b) indicates that the measured end correction agrees with existing theory for thin-walled open pipes. Equating the cross-sectional area of the square pipe to a circular area to determine an effective pipe radius, the Helmholtz number for the experimental situation analyzed in Fig. 1(b) is $ka = 0.48$, where k is the wave number. An approximate value for the end correction can be calculated by⁸

$$\delta = a(0.6133 - 0.1168[ka]^2), \tag{1}$$

resulting in only a slight difference from the value predicted by Levine and Schwinger for $ka \ll 1$.

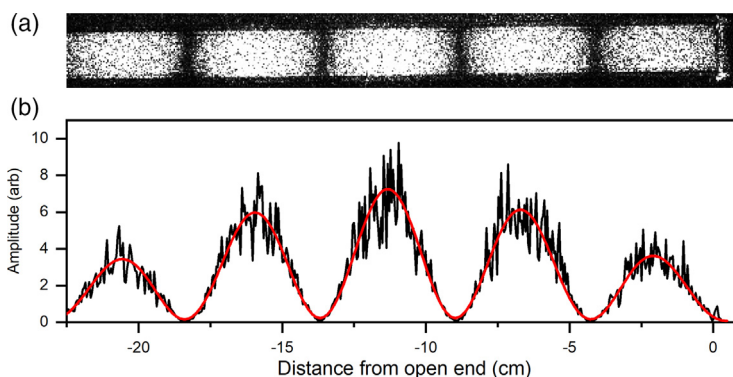


Fig. 1. (a) Image of the final half of the eighth longitudinal mode of the open pipe resonance, where the resonance frequency is 2.90 kHz, (b) average pressure amplitude plotted as a function of position from the end of the pipe. The line represents a nonlinear least squares fit to the measurement.

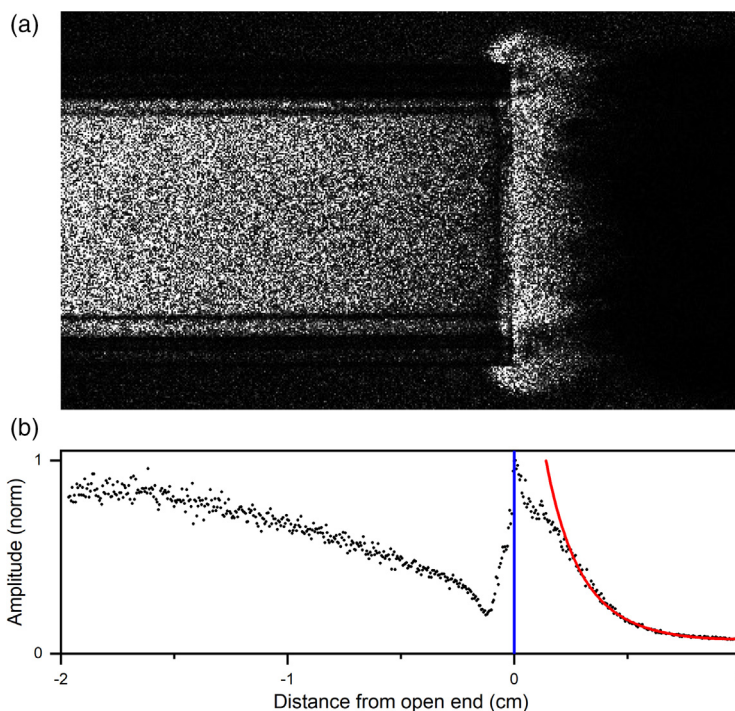


Fig. 2. (a) Image of the standing wave in the final 2 cm of an open pipe oscillating in the fourth longitudinal mode, where the resonance frequency is 1.52 kHz, and (b) average pressure amplitude plotted as a position from the end of the pipe. The vertical line indicates the end of the pipe, and the curve is an exponential fit to the final 8 mm of the detectable standing wave.

The agreement between the measurement of the end correction and the theory is attributable to the end correction being determined by fitting the internal standing wave to a sinusoid, not by measuring the distance from the end of the pipe to a clearly defined final node. Making a measurement of the extension of the standing wave beyond the pipe end is difficult because the decay of the standing wave beyond the pipe end is exponential and not sinusoidal, although there does appear to be a transition region that is neither exponential nor sinusoidal. While it is sometimes assumed that the amplitude of the portion of the standing wave that exists outside of the pipe is a continuation of the sinusoidal dependence inside, the results shown in Fig. 2(b) indicate that this is not the case. Indeed, because the end correction is attributable to the nonzero phase of the atmospheric impedance, it is not obvious that the standing wave should continue beyond the end of the pipe. The fact that the standing wave is found outside of the pipe and the amplitude decays exponentially with distance are phenomena that require further investigation.

More surprising than the existence of the exponentially decaying standing wave beyond the end of the pipe is the unexpected node occurring inside the pipe close to the end. To ensure that this node is not an artifact of the optical system, the flow was imaged by subtracting the images obtained after the flow reached steady-state from an image obtained before the flow began.^{7,9} The resulting series of images have fringes representing the change in optical path length through the flow as depicted in Fig. 3. These fringes oscillate at the acoustic frequency as the pressure in the standing wave varies periodically, and the direction of the motion indicates whether the pressure is increasing or decreasing. The video in Mm. 1 is an example of this type of interferogram and was obtained with a frame rate of 9.9 kHz and played back at a frame rate of 10 Hz. The video shows that the vertical direction of the periodic motion of the fringes in the flow changes direction at the position of the final node inside the pipe in Fig. 2(a), indicating that the amplitude of the pressure variations are indeed π out of phase on either side of the node.

Mm. 1. High-speed TESPI video showing the oscillation of fringes due to the periodic variation in pressure of the standing wave. The direction of the fringe motion indicates whether the pressure is increasing or decreasing. The point at which the vertical motion of the fringes changes direction indicates a node in the standing wave. This is a file of type “mp4” (3.8 kB).

The use of Freon as the gas instead of air appeared to have no influence on the sound other than to decrease the resonance frequencies. However, to ensure that the presence of the final internal node and exponential decay of the pressure amplitude outside of the pipe are not attributable to the gas being Freon, the experiment was repeated using air. When using air, the signal-to-noise ratio (SNR) is significantly lower than when using Freon, but by cooling the air, it is possible to image the standing wave at the end of the pipe with clarity. A plot of the average pressure amplitude in the

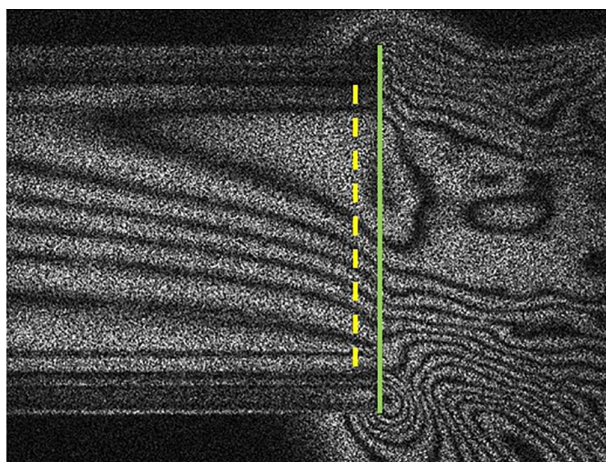


Fig. 3. Subtracted TESPI image of the flow from the end of the pipe. The lines are fringes of equal optical path length imaged through the flow. The solid vertical line represents the end of the pipe, and the dashed line indicates the position of the final internal node. This is a single frame from video [Mm. 1](#), where the position of the π phase shift in the pressure oscillations can be determined to be at the position of the dashed line by the change in the direction of motion of the fringes.

pipe using air as the flowing gas is shown in Fig. 4. The final internal node and exponential decay are evident in spite of the low SNR. Experiments with air at ambient temperature also show the presence of the node before the end of the pipe, but the SNR is too low to accurately fit an exponential decay to the region beyond the pipe end. Additionally, experiments with cylindrical pipes also show similar results, indicating that the presence of the final node inside the pipe as well as the exponential decay of the standing wave beyond the pipe end is independent of the shape of the pipe.

To our knowledge, the presence of a final nonperiodic node and the exponential decay of the standing wave beyond the pipe end have not been reported in the literature. However, there are two issues that may account for this lacuna. First, we can find only one measurement of the standing wave outside of the pipe,¹⁰ hence, the appropriate experiments may not have been performed. Additionally, to detect the final internal node with a microphone, the positioning must be precise and the resolution must be on the order of 1 mm or less.

The second possible explanation for the lack of a previous observation is that the experiments reported here did not include standing waves at the lowest resonance frequencies. It was difficult to force the oscillations associated with the lowest order modes using the fipple that was 3D printed, therefore, the observations reported here are of high-order longitudinal modes. Previous investigations have typically investigated the fundamental mode or a few of the lowest order modes. In no case was there any indication of a higher-order transverse mode, indicating that the internal wavefronts were planar in all of the experiments, but we were unable to produce standing waves below the fourth longitudinal mode of the pipe using either air or Freon.

It is disappointing that currently there appears to be no physical explanation for these observations. However, there are indications in the literature that the behavior may be expected. At least one report of simulations of an open pipe resonating at frequencies well above the fundamental frequency appears to predict the presence of the internal node near the end of the pipe.⁴ Because the purpose of this investigation was to develop computational methods, there was no comment on the shape of the predicted standing wave under the conditions described here. The presence of the anomalous node was noted in the simulations with high flow rates and high-order radial modes; however, Fig. 3 of Ref. 4 indicates the presences of an internal node near the pipe end when a high-order longitudinal mode with planar wavefronts is

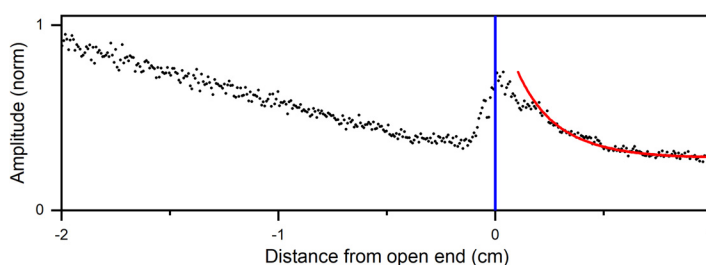


Fig. 4. Average pressure amplitude plotted as a position from the end of the pipe. The gas driving the oscillation was air, and the frequency of oscillation was 1.85 kHz. The vertical line indicates the end of the pipe. The curve is an exponential fit to the final 8 mm of the detectable standing wave.

simulated without flow. Other recent reports of simulations do not predict the presence of a spatially nonperiodic node,⁵ and the final internal node is not predicted for a pipe oscillating in the fundamental mode in either simulation.

Extensive experimental and computational work may be required before the behavior of an acoustic standing wave at the end of an open pipe is fully understood. Experimental observations of standing waves driven by a speaker may lend insight into the process but, unfortunately, we have found it difficult to image the standing wave in this configuration using TESPI. When the standing wave in the pipe is driven by a speaker, the Freon near the end is expelled from the pipe, and the pressure amplitudes of the standing waves created by the speaker are not sufficiently high to observe them in air. Therefore, by necessity, the results presented here are in the presence of flowing gas.

Now that these effects have been observed using TESPI, and it appears likely that they occur with higher-order modes that are seldom investigated, future investigations with microphones may find that they are detectable in air at lower acoustic amplitudes. These experimental investigations combined with further numerical simulations should lead to a better understanding of the complicated behavior of standing waves in open pipes.

Acknowledgments

This research was supported by National Science Foundation Grant No. 2109932.

References and links

- ¹L. Rayleigh, *Theory of Sound* (Dover, New York, 1945), Vol. II, p. 201.
- ²H. Levine and J. Schwinger, "On the radiation of sound from an unflanged circular pipe," *Phys. Rev.* **73**(4), 383–406 (1948).
- ³J. P. Dalmont, C. J. Nederveen, and N. Joly, "Radiation impedance of tubes with different flanges: Numerical and experimental investigations," *J. Sound Vib.* **244**(3), 505–534 (2001).
- ⁴R. Kirby and W. Duan, "Sound radiation from the open end of pipes and ducts in the presence of mean flow," in *Proceedings of ACOUSTICS 2017 Perth*, edited by T. McMinn and A. Duncan, annual Conference of the Australian Acoustical Society (November 19–22, 2017) (AAS, Perth, Australia).
- ⁵V. Hruska and P. Dlask, "Revisiting the open-end reflection coefficient and turbulent losses in an organ pipe with low mach number," *Arch. Acoust.* **46**(1), 197–204 (2021).
- ⁶A. R. da Silva, G. P. Scavone, and A. Lefebvre, "Sound reflection at the open end of axisymmetric ducts issuing a subsonic mean flow: A numerical study," *J. Sound Vib.* **327**, 507–528 (2009).
- ⁷T. R. Moore, L. Baquerizo, Q. Fuse, and M. S. Kellison, "Imaging acoustic standing waves in the presence of flowing gas," *Appl. Opt.* **62**(1), 46–49 (2023).
- ⁸P. Davies, J. L. B. Coelho, and M. Bhattacharya, "Reflection coefficients for an unflanged pipe with flow," *J. Sound Vib.* **72**, 543–546 (1980).
- ⁹T. R. Moore, "Visualization of exhaled breath by transmission electronic speckle pattern interferometry," *Appl. Opt.* **60**(1), 83–85 (2021).
- ¹⁰A. Miklos and J. Angster, "Properties of the sound of flue organ pipes," *Acust. Acta united Ac.* **86**, 611–622 (2000).